First-principles study of low-index surfaces of the Al5Co2 Complex Metallic Alloy

Sebastian Alarcón, Jean-Marie Dubois, Emilie Gaudry

First-principles study of low-index surfaces of the Al_5Co_2 Complex Metallic Alloy

Journal:	*Philosophical Magazine & Philosophical Magazine Letters*
Manuscript ID:	TPHM-10-May-0219.R1
Journal Selection:	Philosophical Magazine
Date Submitted by the Author:	19-Jul-2010
Complete List of Authors:	Alarcón, Sebastian; Institut Jean Lamour, Chimie et Physique des Solides et des Surfaces Dubois, Jean-Marie; Institut Jean Lamour, Chimie et Physique des Solides et des Surfaces Gaudry, E; Institut Jean Lamour, Chimie et Physique des Solides et des Surfaces
Keywords:	surfaces, first-principles calculations, electronic structure
Keywords (user supplied):	Al5Co2 , complex metallic alloy

Philosophical Magazine
Vol. 00, No. 00, july 2010, 1–12

RESEARCH ARTICLE

First-principles study of low-index surfaces of the Al_5Co_2 Complex Metallic Alloy

S. Alarcón Villaseca[a], J.-M. Dubois[a] and É. Gaudry[a*]

Institut Jean Lamour (UMR 7198, CNRS, Nancy-Université, UPV-Metz), département CP2S, Ecole des Mines, Parc de Saurupt, 54042 Nancy cedex, France

(*20 mai 2010*)

The atomic and electronic structures of the (100) and (001) surfaces of the Al_5Co_2 complex metallic alloy are studied by *ab initio* calculations. The relative stability of the possible surface planes built from bulk truncation is calculated and the influence of the atomic surface density, the interlayer spacing and the surface chemical composition on the plane selection is discussed. In addition, we show that the simulated images of scanning tunneling microscopy for each possible termination present a specific signature that appears to be sufficient to experimentally identify the surface plane.

Keywords: Surfaces, First-principles calculations, Electronic structure, Al_5Co_2, Complex metallic alloy.

1. Introduction

Since their discovery by Shechtman *et al.* in 1984 [1], quasicrystals have attracted much interest in the scientific community. Physical and chemical properties have been studied in relation to their unusual symmetries, and innovative applications are expected in various domains [2], particularly in surface coating, due to their specific surface properties [3–8]. Since complex metallic alloy (CMA) phases present a periodic structure which is closely related to the one of their parent quasicrystals, they are then useful, as models ~~of the quasicrystalline phases~~ to catch the key features of the more complex quasicrystalline phases [9–11].

The knowledge of the atomic and electronic surface structures of quasicrystals and/or CMAs is essential for the understanding of their attractive surface properties. However, the determination of the atomic and electronic surface structures in such complex alloys is not simple. In single metals, it is well known that the surface structure might differ from the ideal model built from truncation of the bulk structure due to interlayer relaxations, and sometimes reconstructions. In alloys, additional phenomena may occur such as chemical surface segregation or surface plane selection. These phenomena are driven by the minimization of the surface free energy, defined as the excess free energy per unit area at the surface of a material compared to the bulk [12]. Experimentally, the determination of the surface energy is difficult. The most usual methods are based on the Young equation [13]. A theoretical approach to determine the relative stability of the different possible surface planes is then fundamental to analyze the plane selection that occurs in

*Corresponding author. Email: Emilie.Gaudry@ijl.nancy-universite.fr

ISSN: 1478-6435 print/ISSN 1478-6443 online

DOI: 10.1080/1478643YYxxxxxxxx
http://www.informaworld.com

quasicrystals and their related phases [14–25]. Many factors may have an influence on the surface energy. Among them, atomic densities, interlayer spacing (or gaps between planes in the case of quasicrystals) and chemical composition are key parameters [20]. To study the relative influence of these factors, we have chosen to study two different low-index surfaces of the Al_5Co_2 alloy, which is an approximant of the decagonal phase [26]. The crystal structure of Al_5Co_2 belongs to the space group $P6_3/mmc$ ($hP28$) [27, 28]. Although this aluminide cannot be stricly identified as a usual *sp* Hume-Rothery alloy (it contains transition metal atoms), its electronic structure presents a low density of states (DOS) near the Fermi energy E_F, leading to the formation of a valley in the DOS called a pseudogap that contributes to the alloy stability [29–31]. It is now well established that the formation of this pseudogap is due to the electron diffraction by Bragg planes combined with *sp-d* hybridization [29, 31].

In this paper, we present a theoretical analysis of the atomic and electronic structures of the (100) and (001) surfaces. Along both crystallographic directions Al_5Co_2 is described by a sequence of flat and puckered layers. Perpendicular to the [100] direction, two types of planes of different atomic surface densities alternate, a feature which is also found in orthorhombic $Al_{13}Co_4$ and monoclinic $Al_{13}Fe_4$ CMAs [28, 32, 33]. Perpendicular to the [001] direction, Al_5Co_2 presents two types of planes with the same surface atomic density, but with different chemical compositions. The study of these two kinds of low-index surfaces may help to identify the key parameters responsible for the surface stability. The method used in this paper is based on density functional theory (DFT).

2. Computational details

Structural optimizations and electronic structure calculations have been performed within the density functional theory framework, using the plane-wave Vienna *ab initio* simulation package VASP [34, 35]. Our calculations employ the PAW-PBE pseudopotentials [36–39].

Although the present calculations are called *ab initio*, there are convergence parameters linked to the numerical implementation of the density functional theory framework. Two of them are the plane-wave cutoff energy E_{cut} and the density of k-points sampling the Brillouin zone. A set of test calculations on bulk Al_5Co_2 (28 atoms/cell) has been performed to determine the values of E_{cut} (350 eV) and the size of the Monkhorst-Pack k-points mesh (6×6×6) to achieve a targeted precision for the total energy smaller than 5 meV/atom. A similar k-grid mesh was used for calculations using slabs (6×6×1 for the (001) surface and 1×4×6 for the (100) surface).

The optimization of the atomic coordinates and unit cell parameters was performed by minimization of the Hellmann-Feynman forces acting on the atoms *via* a conjugate gradient algorithm. At the end of the *ab initio* energy minimization, the forces sustained by atoms were less than 0.01 eV/Å. Simulations on the surfaces of Al_5Co_2 were achieved by building symmetric slabs, made of a stack of atomic layers, for each kind of surface terminations. Different thicknesses of slabs were used in this work: 7-layers thick slabs for the puckered (100) and (001) surface terminations, 9-layers thick slab for the flat (001) surface termination. A thinner 5-layers thick slab for the flat (100) surface was used due to the large number of atoms in the slab. A set of test calculations on the flat (001) surface has been performed to evaluate the influence of the slab thickness on the calculated energies. It appears that the surface energy difference between a 5-layers and a 9-layers thick slab is

less than 3 mJ.m^{-2}, while the surface energy difference between a 9-layers and a 13-layers thick slab is less than 1 mJ.m^{-2}. The slabs are separated by a vacuum thickness of 15 Å. The surface lattice parameters were set in agreement with the lattice parameters of the bulk alloy. Atomic relaxation has been performed by allowing displacement of all atoms within the slab except those lying in the central atomic layer.

3. Results and discussion

The experimental lattice parameters of bulk Al_5Co_2 are $a = 7.67$ Å and $c = 7.61$ Å [28]. Geometry optimization calculations for bulk Al_5Co_2 lead to lattice parameters in good agreement with the experimental data: $a = 7.67$ Å, $c = 7.59$ Å. Total energy calculations yield a formation energy equal to $\Delta H_f = -0.47$ eV/atom, which is also in good agreement with the calculated value given by Ref. [40] (-0.48 eV/atom) as well as the experimental data (-0.43 eV/atom) [41].

Figure 1 shows the Al_5Co_2 atomic structure along the [001] and [100] directions. Two kinds of atomic layers are stacked when viewed along both directions: flat-type (F-type) and puckered-type (P-type) atomic layers. Perpendicular to the [100] direction, the two types of planes present different atomic densities: the F-type surface unit cell contains 8 Al atoms and 4 Co atoms, while the P-type surface unit cell contains 12 Al atoms and 4 Co atoms. ~~This leads to an atomic density of about 0.16 at/Å^2 for the P type surface and of about 0.12 at/Å^2 for the F type surface.~~ Perpendicular to the [001] direction, the two types of planes present the same atomic density ~~(about 0.14 at/Å^2)~~, but different chemical compositions: 7 Al atoms for the P-type surface plane and 4 Co + 3 Al atoms for the F-type surface plane. From this structural bulk model, and for each direction considered, two different kinds of surface terminations can be obtained by bulk truncation: F-type and P-type topmost layers.

3.1. *Energetics*

The relative energies of surfaces with different stoichiometries cannot be evaluated directly by comparing the total energies of the corresponding slabs. We thus follow the methodology described in Refs. [12, 42, 43], where the surface energy γ^α of a given surface α is calculated as a function of the chemical potential μ_{Al} of the Al atom in Al_5Co_2:

$$2A\gamma^\alpha = E^\alpha_{slab} - \mu_{Al}N_{Al} - \mu_{Co}N_{Co} \quad (1)$$

where A is the surface area, μ_{Al} (respectively μ_{Co}) is the chemical potential of the Al (respectively Co) atom and N_{Al} (respectively N_{Co}) is the number of Al (respectively Co) atoms. Since Al_5Co_2 is a stable alloy ($\Delta H_f = \mu^{bulk}_{Al_5Co_2} - 5\mu^{bulk}_{Al} - 2\mu^{bulk}_{Co} < 0$), the chemical potentials μ_{Al} and μ_{Co} in Al_5Co_2 have to be smaller than the corresponding μ^{bulk}_{Al} and μ^{bulk}_{Co} in the elemental bulk system, leading to the range of variation of μ_{Al}: $\frac{\Delta H_f}{5} < \mu_{Al} - \mu^{bulk}_{Al} < 0$.

Figure 2a shows the surface energy differences between the F-type and P-type surface planes as a function of μ_{Al} for the two kinds of orientations considered. From Fig. 2a, it appears that the most stable (100) and (001) surface terminations are the P-type atomic planes.

In single metals, the anisotropy of the surface energy as a function of the ori-

entation is explained by the "broken bonds" model, that states that the surface energy is proportional to the product of the number of broken bonds times the bonding energy [44, 45]: the densest atomic planes, whose atoms are surrounded by the most complete environment, presents the lowest surface energy. In Al_5Co_2, the situation is more complex, since all atoms in bulk Al_5Co_2 do not have the same kind of environment, contrary to what happens in simpler metals. The atoms in bulk Al_5Co_2 occupy five types of inequivalent sites. One can then define five types of clusters surrounding each atom in the structure [27] (see Tab. 1). The creation of the (100) surface induces the break of the same number of bonds ~~(0.61 bonds per Å^2)~~ for both P-type and F-type terminations although the densities of both terminations differ. The formation of the (001) surface leads to the break of ~~0.59 bonds per Å^2~~ 30 bonds in the surface unit cell for the P-type termination and only ~~0.53 bonds per Å^2~~ 27 bonds in the surface unit cell for the F-type termination, altough these two terminations present the same ~~surface atomic density~~ number of atoms in the surface unit cell. For both (100) and (001) low-index surfaces, a simple relation between the number of broken bonds in the first environment of each atom and the surface energy seems then difficult to obtain. Indeed, in such a complex metallic alloy, some of the Al-Co bonds may have enhanced covalency and therefore all broken bonds may not contribute to the surface energy in the same way [46].

Another parameter that influences the surface energy is the chemical composition of the surface layer. When comparing the stabilities of the two (001) terminations it appears that the most stable termination, among the two topmost surfaces with the same atomic density considered, is the Al-rich atomic plane. An interpretation of this result is the presence of cobalt atoms in the (001) F-type surface plane: the elementary surface energy of cobalt (2.522 J.m^{-2} [47], 2.550 J.m^{-2} [41]) is higher than that of aluminium (1.143 J.m^{-2} [47], 1.160 J.m^{-2} [41]). The presence of cobalt atoms in the topmost layer is unfavoured, the low-density (100) surface with a surface cobalt atomic composition of 33% being more stable than the denser F-type (001) surface (surface cobalt atomic composition of 57%).

It is interesting then to compare the surface energies of the Al_5Co_2 CMA to the more simple AlCo alloy. In the case of the (110) surface of AlCo, all planes are equivalent and the surface energy can be deduced from the equation used to calculate the surface energy in single metals: $\gamma = \frac{1}{2A}(E^{slab} - NE^{bulk})$ where E^{slab} is the total energy of the symmetric slab considered, E^{bulk} is the total energy of the corresponding bulk and N is the number of layers considered in the slab. In this approach, we consider a perfect (110)AlCo surface, we do not consider the deviation from the bulk stoichiometry in the second layer as highlighted by Ref. [48]. However, our results for the interlayer distances and the surface rippling are in good agreement with the experimental data: we found a rippling for the topmost layer of 0.19 Å (0.18 Å from Ref. [48]) and an interlayer distance $d_{12} = 2.04$ Å (2.04 Å from Ref. [48]). The surface energy calculated for (110)AlCo (2.07 J.m^{-2}) is higher than the (100) surface energies calculated for the two considered terminations. This confirms that the presence of Co atoms at the surface is unfavoured: (100) F-type Al_5Co_2 presents a surface atomic density much lower than (110)AlCo, but the (110)AlCo contains much more Co surface atoms.

3.2. *Electronic structure*

Figure 2b shows the calculated local density of states (LDOS) on surface and subsurface planes for the Al_5Co_2(001) slab with F-type termination. The results

for the bulk calculations are in good agreement with previous studies [29–31].

The effect of the surface is mainly confined to the two topmost surface layers. Concerning the F-type termination, the Co-3*d* band width of the surface layer is slightly reduced by about 0.2 eV compared to the bulk. The Co *d*-band is also shifted by about 0.4 eV towards lower binding energies compared to the corresponding bulk "F-type" Co *d*-band. These effects are attributed to the reduction in the coordination number of surface atoms compared to the bulk. Similar shifts of the calculated transition metal *d*-band center of mass of the surface DOS have also been reported for the tenfold surface of the *d*-Al-Ni-Co quasicrystal ($\simeq 0.8$ eV) and for the fivefold surface of the *i*-Al-Pd-Mn quasicrystal ($\simeq 0.5$ eV) [9, 10].

A noteworthy feature in the density of states is the existence of a pseudogap at the Fermi level E_F of the bulk material: $n(E_F) = 0.11$ states/eV/atom, in agreement with the value of Trambly *et al.* (0.13 states/eV/atom [29]). Concerning the F-type (001) surface, the pseudogap is hardly noticeable on the DOS of the topmost atomic layer, while it appears in the next subsurface atomic layers. This behaviour is in agreement with the shallower surface pseudogap calculated on the fivefold surface of *i*-Al-Pd-Mn quasicrystal [11]. However, the decrease of the pseudogap depth is much more pronounced in the latter case.

3.3. *Simulated STM images*

STM images are simulated within the Tersoff-Hamann approximation [49, 50]. The calculated images are shown in Fig. 3 for each type of surface termination ($V_{bias} = 0.7$ V, $d_{tip-surface} = 3$ Å).

3.3.1. The Al_5Co_2 (001) surface

The STM image corresponding to the Al-rich termination shows lines of bright triangles. This contrast is due to the presence of three Al atoms slightly above ($\simeq 0.44$ Å) the mean position of the plane. The other Al atoms, at $\simeq 0.12$ Å and $\simeq 0.41$ Å underneath the mean position of the atomic plane contribute to the dark contrast in the STM image.

The STM image corresponding to the F-type termination shows similar triangles although connected to each other by a bright spot. The bright constrast of the triangle is due to the 3 Al atoms slightly ($\simeq 0.15$ Å) above the mean position of the atomic plane. The bright spot connecting the triangles is due to the Co atom situated at about the same z-position as the 3 Al atoms. The other three Co atoms slightly underneath the mean position of the topmost atomic plane, do not appear in the STM image.

3.3.2. The Al_5Co_2 (100) surface

The STM image of the F-type termination shows very bright spots aligned along the [001] direction and a rather bright zig-zag feature. The contrast of the brightest spots are due to Al atoms at the mean position of the atomic plane. The contrast of the zig-zag feature is due to the six remaining Al atoms slightly above the mean position of the atomic plane and to the two Co atoms slightly below the mean position of the atomic plane. The two remaining Co atoms are about 0.28 Å below the mean position of the atomic plane, they do not contribute to the bright contrast of the STM image.

In the case of the P-type termination, we can observe sequences of zig-zag rows of bright pentagons. The pentagonal features are due to the Al atoms ~~slightly~~ above the mean position of the topmost atomic plane (about 0.26-0.29 Å), that are

arranged in pentagonal features. The center of the pentagons is occupied by a Co atom underneath the mean position of the plane (about 0.51 Å). The simulated STM image shows also lines of grey contrast, which is due to a Co atom ~~slightly~~ above the mean position of the plane (about 0.22 Å).

4. Conclusion

The atomic and electronic structures of the (100) and (001) surfaces of the Al_5Co_2 CMA have been studied by *ab initio* calculations.

Among the three main factors influencing the surface energy and the selection of the surface plane in complex metallic alloys [20], the interlayer spacing does not seem to play a major role here since it is the same for the two energetically different terminations considered for a given low-index surface. The comparison of the stability of the two surface structures with the same number of atoms in the surface unit cell - the (001) surface - shows that the Al-richer atomic layer is preferred as surface termination. The comparison of the stability of the two surface structures with close atomic compositions (25% or 33% at. Co for the two considered terminations of the (100) surface) shows that the denser atomic layer is preferred as surface termination. However, the influence of the atomic density, which is not always directly related to the number of broken bonds in such a complex alloy, is difficult to highlight rigorously, since in the examples considered here, one cannot set stricly apart its influence from the influence of the atomic composition. The comparative study of the four considered surface models shows that the surface energy and the percentage of Co surface atoms increase in the following sequence: (100) P-type termination, (100) F-type termination, (110)AlCo surface, (001) F-type termination. The atomic composition seems then to have a significant impact on the surface plane selection, the presence of Co surface atoms being unfavoured.

In this paper, we have also shown that the determination of the electronic structure of each surface leads to a specific STM image: the differences between the two considered topmost layers appear to be sufficient to identify the surface plane by scanning tunneling microscopy. Experimentally, studies of the Al_5Co_2 (100) surface would be interesting, but the synthesis of a millimeter-sized sample is difficult, since (i) this phase is formed during a peritetic reaction at a temperature higher than 1400 K, (ii) it requires a narrow temperature range for the crystal growth (about 50^oC), combined with a narrow composition range for the Al_5Co_2 phase ($\pm$ 3%at Al composition). However, it might be worth: since the stable (100) termination built from bulk truncation (P-type surface) contains Co surface atoms, one may expect an attractive behaviour for catalysis applications.

5. Acknowledgements

The European Network of Excellence on "Complex Metallic Alloys" (NMP3-CT-2005-500145), and the "Agence Nationale de la Recherche" (ANR-08-BLAN-0041-01) are acknowledged for their financial support. Computing time was partially supplied by the "Institut Français Développement et de Recherche en Informatique Scientifique" in Orsay (project 99642). One of us (SAV) thanks INC-CNRS and the "Région Lorraine" for financial support during his PhD thesis.

References

[1] D. Shechtman, I. Blech, D. Gratias and J. Cahn, Phys. Rev. Lett. 53 (1984) p.1951.
[2] J.-M. Dubois, *Useful quasicrystals*, World Scientific Pub Co Inc, (2005).
[3] T. Tanabe, S. Kameoka and A. Tsai, Catalysis Today 111 (2006) p.153.
[4] A. Tsai and M. Yoshimura, Applied Catalysis 214 (2001) p.237.
[5] M. Yoshimura and A. Tsai, J. Alloys Comp. 342 (2002) p.451.
[6] B.P. Ngoc, C. Geantet, M. Aouine, G. Bergeret, S. Raffy and S. Marlin, International Journal of hydrogen energy 33 (2008) p.1000.
[7] C. Jenks and P.A. Thiel, Journal of Molecular Catalysis A: Chemical 131 (1998) p.301.
[8] J.-M. Dubois, S.S. Kang and J.V. Stebut, Journal of Materials Science Letters 10 (1991) p.537.
[9] M. Krajčí and J. Hafner, Phys. Rev. B 71 (2005) p.054202.
[10] M. Krajčí, , J. Hafner and M. Mihalkovič, Phys. Rev. B 73 (2006) p.134203.
[11] M. Krajčí, and J. Hafner, Phys. Rev. B 80 (2009) p.214419.
[12] F. Bechstedt, *Principles of surface physics*, Springer, Berlin, (2003).
[13] L. Vitos, A. Ruban, H. Skriver and J. Kollár, Surf. Sci. 411 (1998) p.186.
[14] M. Gierer, M.V. Hove, A. Goldman, Z. Shen, S.L. Chang, P. Pinhero, C. Jenks, J. Anderegg, C.M. Zhang and P.A. Thiel, Phys. Rev. B 57 (1998) p.7628.
[15] T. Cai, F. Shi, Z. Shen, M. Gierer, A. Goldman, M. Kramer, C. Jenks, T. Lograsso, D. Delaney, P. Thiel and M.V. Hove, Surf. Sci. 495 (2001) p.19.
[16] L. Barbier, D.L. Floc'h, Y. Calvayrac and D. Gratias, Phys. Rev. Lett. 88 (2002) p.085506.
[17] Z. Papadopolos, G. Kasner, J. Ledieu, E.J. Cox, N.V. Richardson, Q. Chen, R.D. Diehl, T.A. Lograsso, A.R. Ross and R. McGrath, Phys. Rev. B 88 (2002) p.184207.
[18] J. Ledieu and R. McGrath, J. Phys.: Condens. Matter 15 (2003) p.S3113.
[19] R.D. Diehl, J. Ledieu, N. Ferralis, A.W. Szmodis and R. McGrath, J. Phys.: Condens. Matter 15 (2003) p.R63.
[20] B. Unal, C. Jenks and P.A. Thiel, Phys. Rev. B 77 (2008) p.195419.
[21] M. Shimoda, H. Sharma and A. Tsai, Surf. Sci. 598 (2005) p.88.
[22] V. Fournée, A. Ross, T. Lograsso, J. Anderegg, C. Dong, M. Kramer, I. Fisher, P. Canfield and P.A. Thiel, Phys. Rev. B 66 (2002) p.165423.
[23] H. Sharma, M. Shimoda, V. Fournée, A. Ross, T. Lograsso and A. Tsai, Phys. Rev. B 71 (2005) p.224201.
[24] R. Addou, E. Gaudry, T. Deniozou, M. Heggen, M. Feuerbacher, P. Gille, Y. Grin, R. Widmer, O. Groening, V. Fournée, J.-M. Dubois and J. Ledieu, Phys. Rev. B 80 (2009) p.014203.
[25] T. Deniozou, R. Addou, A.K. Shukla, M. Heggen, M. Feuerbacher, M. Krajčí, J. Hafner, R. Widmer, O. Groning, V. Fournée, J.-M. Dubois and J. Ledieu, Phys. Rev. B 81 (2010) p.125418.
[26] S. Song and E. Ryba, Phil. Mag. 65 (1992) p.85.
[27] U. Burkhardt, M. Ellner and J. Grin, Powder Diffr. 11 (1996) p.123.
[28] U. Burkhardt, M. Ellner, J. Grin and B. Baumgartner, Powder Diffr. 13 (1997) p.159.
[29] G.T. Laissardièrede , D.N. Manh, L. Magaud, J.P. Julien, F. Cyrot-Lackmann and D. Mayou, Phys. Rev. B. 52 (1995) p.7920.
[30] E. Belin-Ferré, G. Trambly de Laissardière, P. Pêcheur, A. Sadoc and J.-M. Dubois, J. Phys.: Condens. Matter 9 (1997) p.9585.
[31] G. Trambly de Laissardière, D.N. Manh and D. Mayou, Progress in Materials Science 50 (2005) p.679.
[32] J. Grin, U. Burkhardt, M. Ellner and K. Peters, J. Alloys Comp. 206 (1994) p.243.
[33] J. Grin, U. Burkhardt, M. Ellner and K. Peters, Z. Kristallogr. 209 (1994) p.479.
[34] G. Kresse and J. Furthmller, Phys. Rev. B 54 (1996) p.11169.
[35] G. Kresse and J. Furthmller, Computational Materials Science 6 (1996) p.15.
[36] P.E. Blöchl, Phys. Rev. B 50 (1994) p.17953.
[37] G. Kresse and D. Joubert, Phys. Rev. B 59 (1999) p.1758.
[38] J.P. Perdew, K. Burke and M. Ernzerhof, Phys. Rev. Lett. 77 (1996) p.3865.
[39] J.P. Perdew, K. Burke and M. Ernzerhof, Phys. Rev. Lett. 78 (1997) p.1396.
[40] M. Mihalkovič and M. Widom, http://alloy.phys.phys.cmu.edu.
[41] F. Boerde , R. Boom, W. Mattens, A. Miedema and A. Niessen, *Cohesion in metals* (1988).
[42] N. Moll, A. Kley, E. Pehlke and M. Scheffler, Phys. Rev. B 54 (1996) p.8844.
[43] L. Dias, A. Leitao, C. Achete, R.P. Blum, H. Niehus and R. Capaz, Surf. Sci. 601 (2007) p.5540–5545.
[44] I. Galanakis, G. Bihlmayer, V. Bellini, N. Papanikolaou, R. Zeller, S. Blgel and P.H. Dederichs, Europhys. Lett. 58 (2002) p.751.
[45] I. Galanakis, N. Papanikolaou and P.H. Dederichs, Surf. Sci. 511 (2002) p.1.
[46] M. Krajčí and J. Hafner, Journal of Non-Crystalline Solids, 334-335 (2004) p. 342.
[47] W. Tyson and W. Miller, Surf. Sci. 62 (1977) p.267.
[48] V. Blum, C. Rath, G.R. Castro, M. Kottcke, L. Hammer and K. Heinz, Surface Review and Letters 3 (1996) p.1409.
[49] J. Tersoff and D.R. Hamann, Phys. Rev. B 31 (1985) p.805.
[50] J. Tersoff and D.R. Hamann, Phys. Rev. Lett. 50 (1983) p.1998.

	site	Coord. Nb
Al_1	$2a$	Al_1-6Co
		Al_1-6Al
Al_2	$6h$	Al_2-3Co
		Al_2-10Al
Al_3	$12k$	Al_3-4Co
		Al_3-10Al
Co_1	$2d$	Co_1-9Al
Co_2	$6h$	Co_2-10Al
		Co_2-2Co

Table 1. The coordination numbers of the atoms in bulk Al_5Co_2.

Figure 1. Atomic structure of Al_5Co_2 along the [100] (a) and [001] (b) directions.

Figure 2. (a) Calculated surface energies of the different topmost layers considered in each orientation. The chemical potential μ_{Al}^{bulk} corresponding to fcc aluminium is taken as reference. (b) Densities of states of the surface and sub-surface planes compared to the corresponding bulk DOS for the F-type (001) topmost layer. The label S refers to the surface plane, S-1 to the plane immediately below, etc... The DOS of each surface atomic plane are compared with the DOS of the corresponding atomic plane in the bulk structure.

Figure 3. Simulated STM images corresponding to the (100) and (001) surfaces (V_{bias} = 0.7 V, $d_{tip-surface}$ = 3 Å).

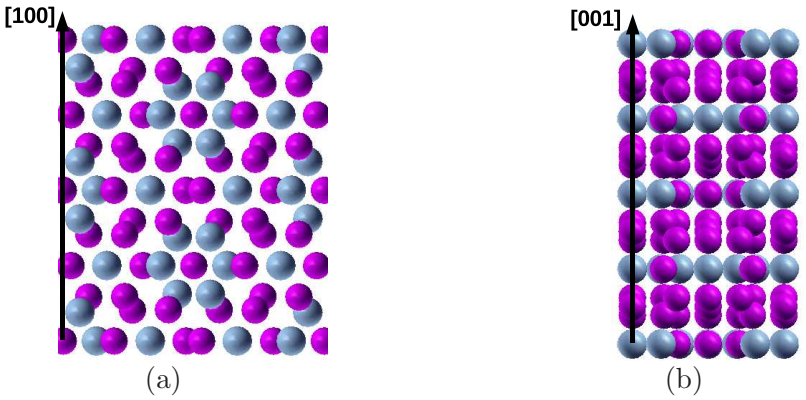

Figure 1. Atomic structure of Al_5Co_2 along the [100] (a) and [001] (b) directions.

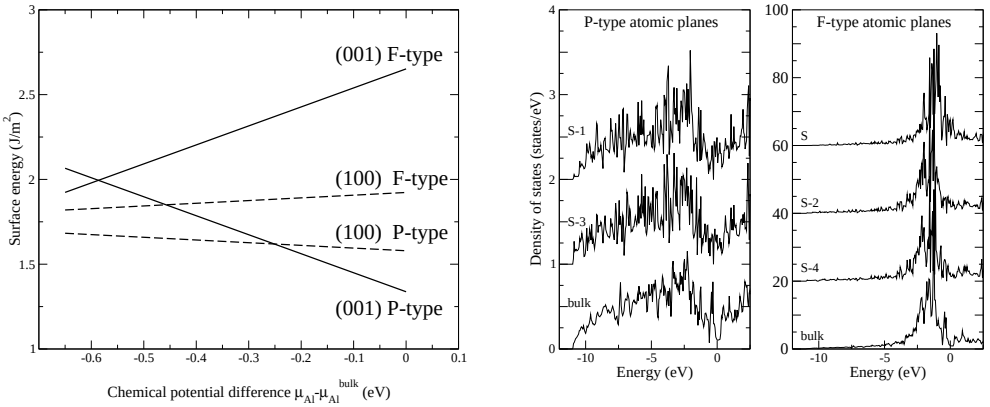

(a) (b)

Figure 2. (a) Calculated surface energies of the different topmost layers considered in each orientation. The chemical potential μ_{Al}^{bulk} corresponding to fcc aluminium is taken as reference. (b) Densities of states of the surface and sub-surface planes compared to the corresponding bulk DOS for the F-type (001) topmost layer. The label S refers to the surface plane, S-1 to the plane immediately below, etc.. The DOS of each surface atomic plane are compared with the DOS of the corresponding atomic plane in the bulk structure.

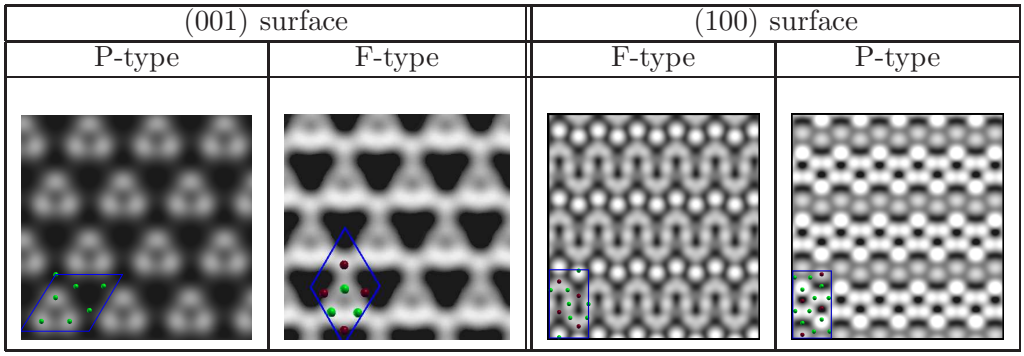

Figure 3. Simulated STM images corresponding to the (100) and (001) surfaces (V_{bias} = 0.7 V, $d_{tip-surface}$ = 3 Å).

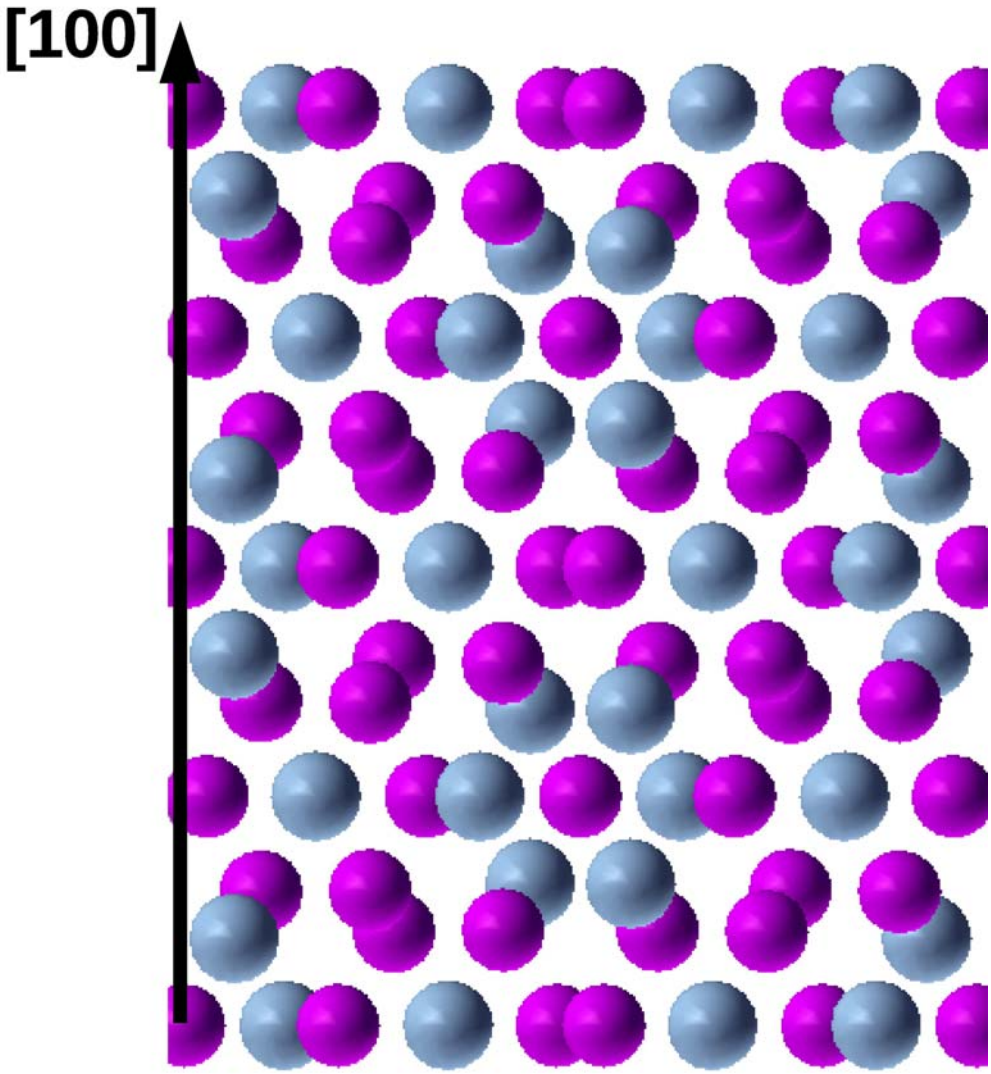

Atomic structure of Al5Co2 along the [100] (a) and [001] (b) directions.

144x160mm (600 x 600 DPI)

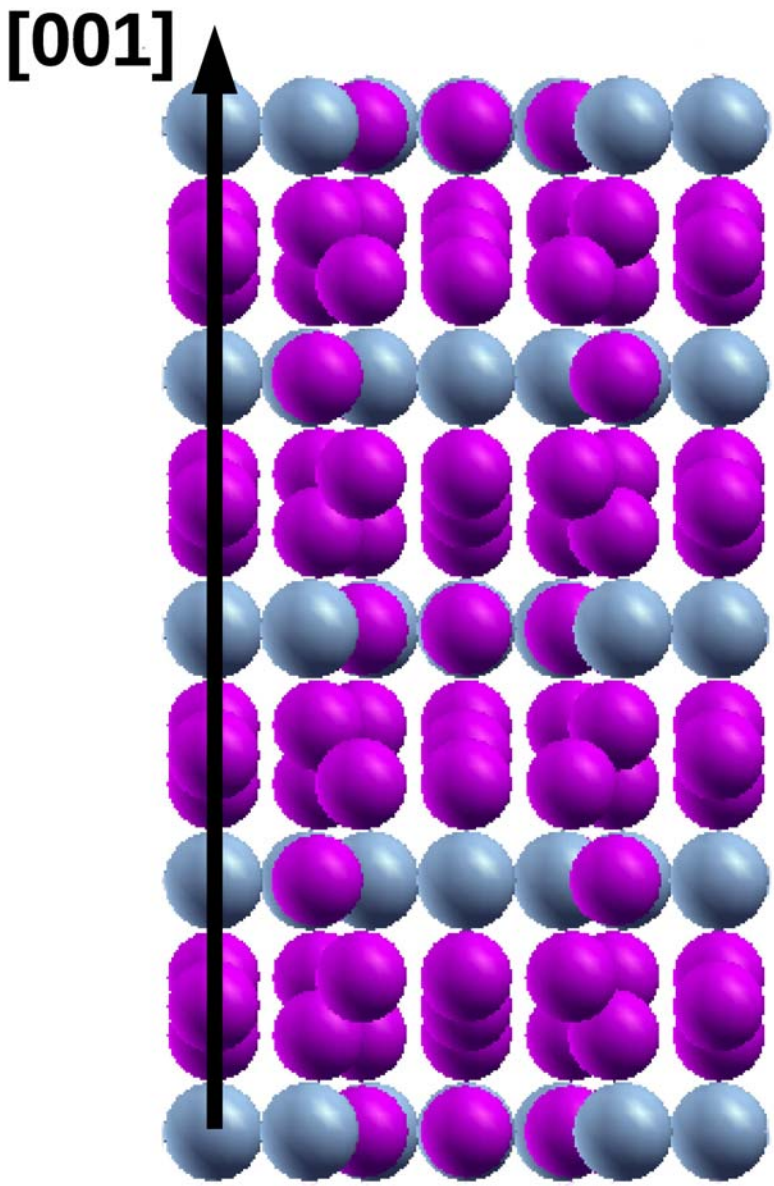

Atomic structure of Al5Co2 along the [100] (a) and [001] (b) directions.

105x157mm (600 x 600 DPI)

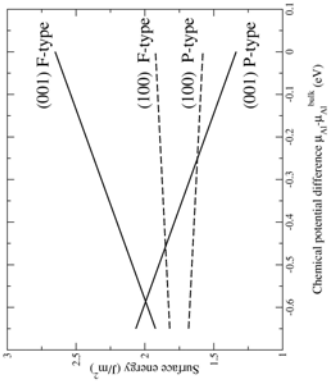

Calculated surface energies of the different topmost layers considered in each orientation. The chemical potential μ_{Al}^{bulk} corresponding to *fcc* aluminium is taken as reference.
215x279mm (600 x 600 DPI)

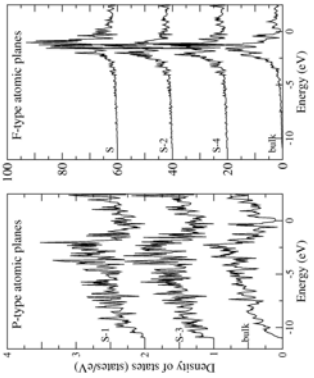

Densities of states of the surface and sub-surface planes compared to the corresponding bulk DOS for the F-type (001) topmost layer. The label S refers to the surface plane, S-1 to the plane immediately below, etc... The DOS of each surface
atomic plane are compared with the DOS of the corresponding atomic plane in the bulk structure.

215x279mm (600 x 600 DPI)

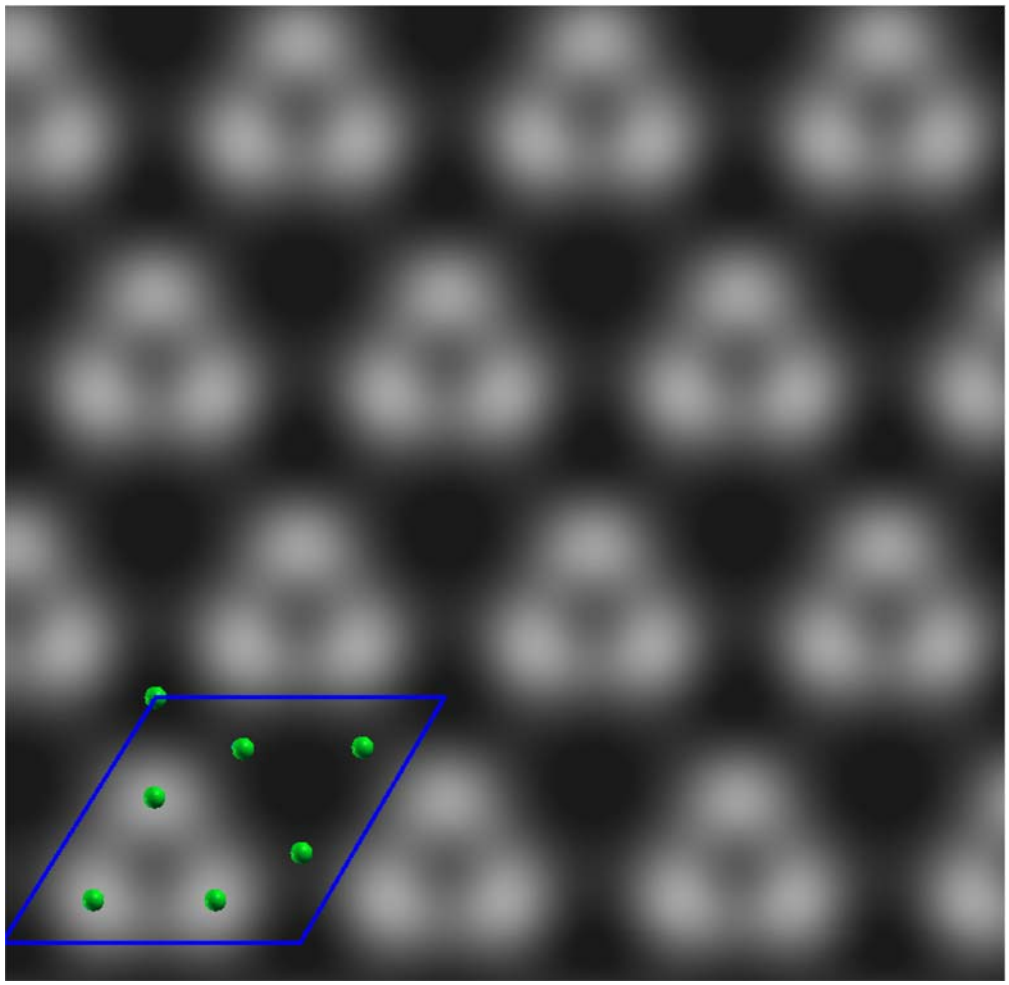

Simulated STM images corresponding to the (100) and (001) surfaces (V_{bias} = 0.7 V, $d_{tip\text{-}surface}$ = 3Å.
254x248mm (600 x 600 DPI)

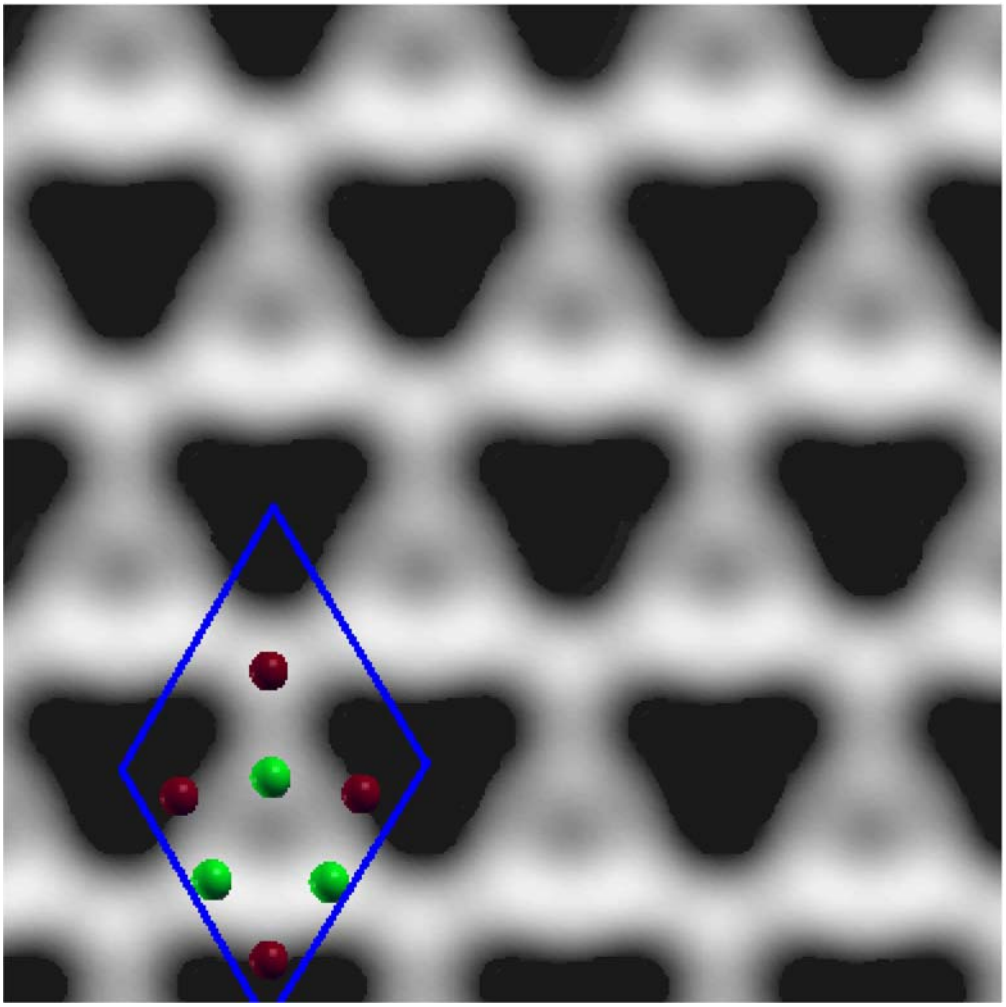

Simulated STM images corresponding to the (100) and (001) surfaces (V_{bias} = 0.7 V, $d_{tip\text{-}surface}$ = 3Å.
137x137mm (600 x 600 DPI)

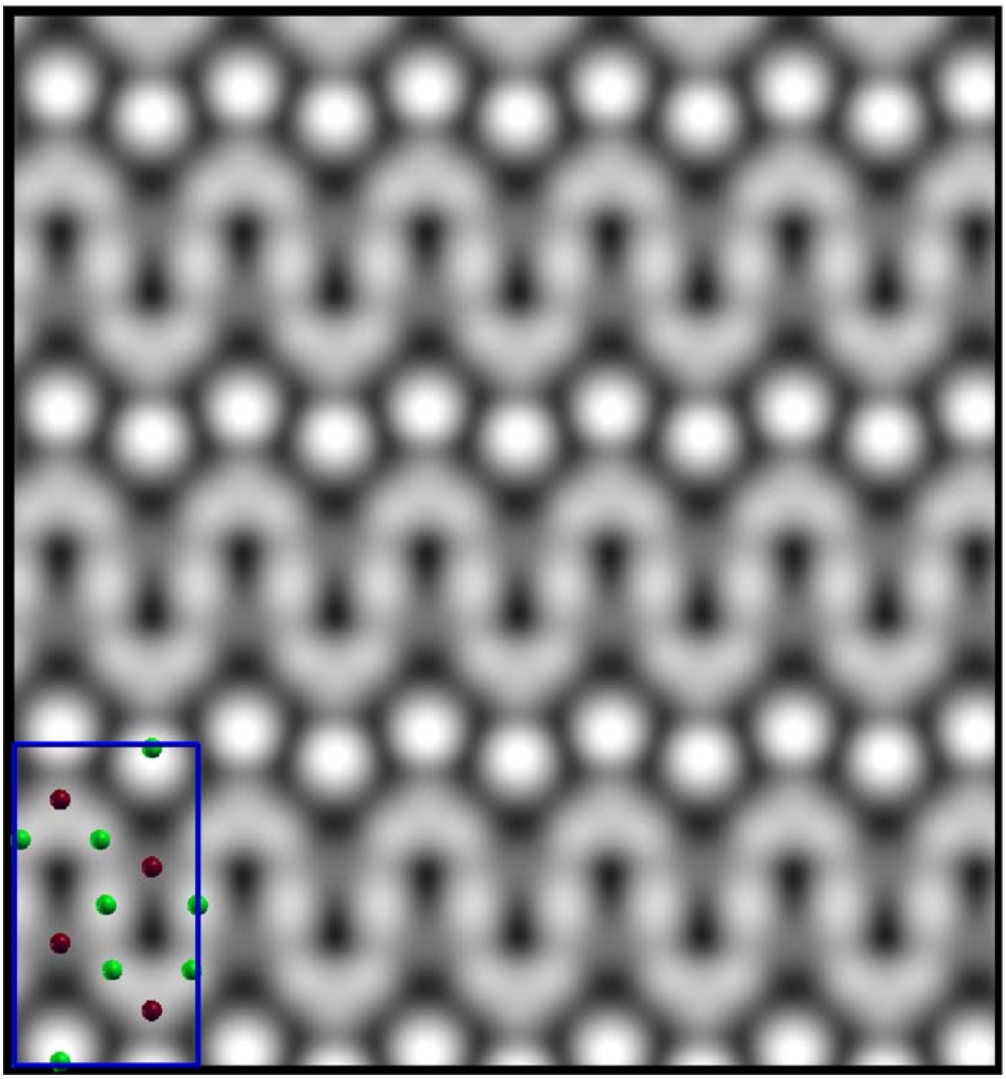

Simulated STM images corresponding to the (100) and (001) surfaces (V_{bias} = 0.7 V, $d_{tip\text{-}surface}$ = 3Å.
187x200mm (600 x 600 DPI)

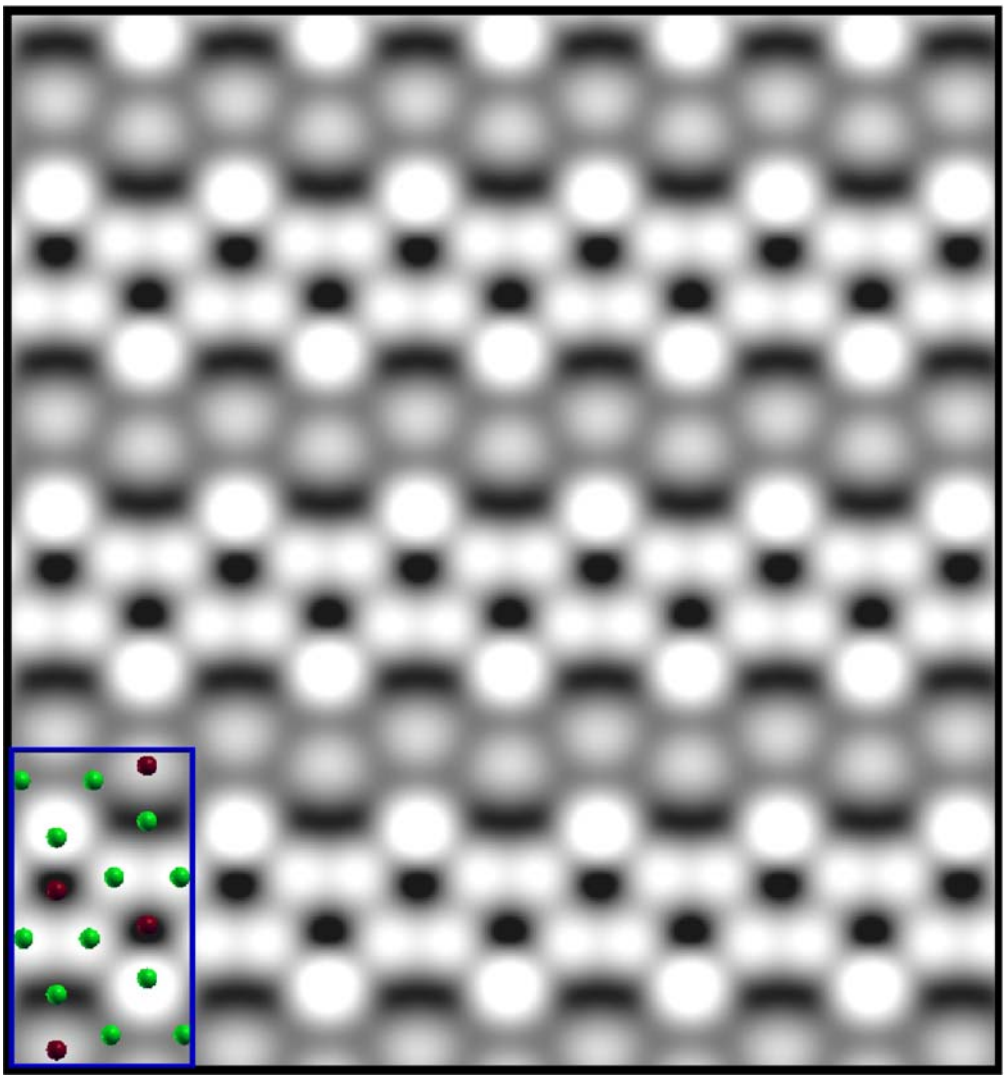

Simulated STM images corresponding to the (100) and (001) surfaces (V_{bias} = 0.7 V, $d_{tip\text{-}surface}$ = 3Å.
187x200mm (600 x 600 DPI)